Remote Sensing of Environment 115 (2011) 1997–2007

Contents lists available at ScienceDirect

Remote Sensing of Environment

journal homepage: www.elsevier.com/locate/rse

Characterizing spatial patterns of invasive species using sub-pixel classifications

A.E. Frazier, L. Wang *

University at Buffalo, the State University of New York, Department of Geography, 105 Wilkeson Quad, Buffalo, NY 14261, USA
National Center for Geographic Information and Analysis (NCGIA), 301 Wilkeson Quad, Buffalo, NY 14261, USA

ARTICLE INFO

Article history:
Received 17 December 2010
Received in revised form 10 March 2011
Accepted 2 April 2011
Available online 8 May 2011

Keywords:
Sub-pixel classification
Spectral unmixing
Saltcedar
Landscape metrics
Threshold continuum

ABSTRACT

Invasive species disrupt landscape patterns and compromise the functionality of ecosystem processes. Non-native saltcedar poses significant threats to native vegetation and groundwater resources in the southwestern U.S. and Mexico, and quantifying spatial and temporal distribution patterns is essential for monitoring its spread. Considerable research focuses on determining the accuracy of various remote sensing techniques for distinguishing saltcedar from native woody riparian vegetation through sub-pixel, or soft classifications. However, there is a lack of research quantifying spatial distribution patterns from these classifications, mainly because landscape metrics, which are commonly used to statistically assess these patterns, require bounded classes and cannot be applied directly to soft classifications. This study tests a new method for discretizing sub-pixel data to generate landscape metrics using a continuum of fractional cover thresholds. The developed approach transforms sub-pixel classifications into discrete maps compliant with metric terms and computes and interprets metric results in the context of the region to explain patterns in the extent, distribution, and connectivity of saltcedar in the Rio Grande basin. Results indicate that landscape metrics are sensitive to sub-pixel values and can vary greatly with fractional cover. Therefore spectral unmixing should be performed prior to metric calculations. Analysis of metric trends provides evidence that saltcedar has expanded away from the immediate riparian zones and is displacing native vegetation. This information, coupled with control management strategies, can be used to target remediation activities along the Rio Grande.

1. Introduction

Invasive species threaten the environment and ecosystem health by disrupting natural landscape patterns and interfering with ecosystem processes (Dukes & Mooney, 2004; Vitousek et al., 1997). Saltcedar (*Tamarix* spp.) is recognized as one of the most invasive vegetation species, particularly across the southwestern United States and Mexico (Morisette et al., 2006). The shrub-like weed persists in drought conditions by outcompeting native vegetation for water resources, but offers fewer benefits to wildlife (Everitt & DeLoach, 1990). Impacts of saltcedar invasion are most pronounced in the Rio Grande basin where limited water supplies are increasingly depleted by its presence. Quantifying spatial and temporal distribution patterns of saltcedar is essential for monitoring and predicting its spread for ecosystem management.

Remote sensing is used extensively for saltcedar detection (Everitt et al., 1996), and classification procedures for differentiating saltcedar from native vegetation are tested rigorously (Everitt & DeLoach, 1990; Groeneveld & Watson, 2008; Hamada et al., 2007; Narumalani et al., 2009; Pu et al., 2008; Silván-Cárdenas & Wang, 2010; Wang & Silván-Cárdenas, under revision). Sub-pixel or soft classification methods, which assign each pixel multiple fractions according to various land covers (Keshava & Mustard, 2002; Roberts et al., 1998; Song, 2005), are often the most expedient means to obtain detailed saltcedar information when high resolution imagery cannot be obtained. Silván-Cárdenas and Wang (2010) tested various sub-pixel classification techniques for saltcedar detection and found that these procedures enhance the utility of Landsat data for tackling the saltcedar invasion problem.

Advances in remote sensing have refined and improved sub-pixel classification methods, but there is a notable lack of research extrapolating spatial pattern information from these soft classifications in order to quantify saltcedar distribution. Research has established that landscape structure patterns influence ecological processes (Bekker et al., 2009; Mas et al., 2010), and these spatial patterns can be measured for remote sensing classifications using landscape metrics (Bekker et al., 2009; Brown et al., 2000; Harold et al., 2005; Kamusoko & Aniya, 2007; Soto et al., 2009; Southworth et al., 2004). Walsh et al. (2008) also found that coupling spectral measurements with metric analysis can provide insight into the process of invasion, yet there are no known studies applying landscape metrics to saltcedar data.

This noted dearth of research is likely due to a computational limitation of landscape metrics in which discrete classes with hard boundaries are required for metric analysis. Sub-pixel classifications, a common approach for saltcedar detection, generate fractional land

* Corresponding author at: University at Buffalo, Geography Department, 105 Wilkeson Quad, Buffalo, NY 14261, USA. Tel.: +1 716 645 0474; fax: +1 716 645 2329.
E-mail address: lewang@buffalo.edu (L. Wang).

0034-4257/$ – see front matter
doi:10.1016/j.rse.2011.04.002

covers. These proportional values form continuously changing land cover gradients across the study area and do not produce discrete class boundaries. Sub-pixel classifications therefore cannot be directly subjected to metric calculations.

A handful of studies have attempted to resolve this issue by reclassifying sub-pixel proportions into hardened regions according to proportional ranges (e.g., 0–0.1, 0.1–0.2, 0.2–0.3, etc.) and computing separate metrics for each range (Rashed, 2008; Van de Voorde et al., 2009; Walsh et al., 2008) without regard for values above or below the range limits. This range method is suitable for analysis of specific proportional ranges but is not optimal for analyzing entire landscapes, especially in the context of invasive species. The degree of spread of an invasive species correlates with local abundance (Affre et al., 2010), and higher degrees of spread have been found to have greater detrimental impacts on native vegetation (deWinton & Clayton, 1996). Based on this logic, it is imperative to include all pixels with fractional cover greater than the chosen threshold when discretizing sub-pixel classifications for metric analyses. These pixels exceedingly satisfy the selected criteria for saltcedar proportion and represent, at minimum, equivalent stress to the system, therefore it is appropriate to include them when computing metrics.

This study tests a new method for discretizing sub-pixel classifications for metric analysis by setting a continuum of fractional cover thresholds and converting continuous cover fractions to discrete cover classes based on fractional cover thresholds. The study subjects multiple sub-pixel classifications to this threshold approach in order to calculate landscape metrics, and interprets metric results to explain spatial and temporal distributions of saltcedar across the study area. The objectives of the research are to (1) compare the Soft Maximum Likelihood Classification (SMLC; Foody et al., 1992) and the Tessellated Spectral Linear Unmixing (TLSU; Silván-Cárdenas & Wang, 2010) techniques for sub-pixel saltcedar detection using a time series of Landsat TM data, (2) test a threshold continuum approach for reclassifying sub-pixel fractional cover from soft classification results in order to calculate landscape metrics, (3) analyze the spatial patterns of saltcedar and interpret them according to the extent, distribution and connectedness of growth across the landscape, and (4) compare saltcedar patterns to native vegetation patterns to determine if coupled landscape structure changes are occurring in the ecosystem.

2. Study area and data

2.1. Study area

The Forgotten River is an approximately 100 km stretch of the Rio Grande, between 30°23′–29°35′N latitude and 104°50′–104°24′ W longitude, that runs along the Mexico–U.S. border and is one of the least researched areas of the entire river system. The study area consists of the vegetated riparian zone on both sides of the river (Fig. 1), comprised mostly of saltcedar with mixes of native willow (*Salix* spp.) and mesquite (*Prosopis* spp.). The climate in the region is semi-arid to arid, with average annual rainfall amounts of less than 30 cm and maximum summer temperatures as high as 40 °C. Topography is characterized by canyons and small valleys with elevation ranging from 700 m to 950 m. In general, water resources in the region are scarce, and the presence of saltcedar exacerbates shortages.

2.2. Image pre-processing

Three Landsat TM images (30-m spatial resolution), acquired from Path 31, Row 39 on 29 December 2000, 8 December 2004, and 3 December 2008, provide the basis for quantifying saltcedar spatial pattern changes over time. Late fall–early winter is the optimal time to distinguish saltcedar from remotely sensed images as the foliage turns a yellow-orange-brown color, and the spectral characteristics are vastly different from the surrounding native vegetation (Everitt & DeLoach, 1990; Everitt et al., 1996).

Landsat TM images were georeferenced to a base Landsat 7 ETM+ image with root mean square errors of 0.011, 0.011 and 0.008 pixels respectively. The ETM+ image was acquired on 19 December 2005, concurrent with the acquisition of an Airborne Imaging Spectroradiometer for Applications (AISA) image on 21 December 2005 obtained for hyperspectral endmember selection. AISA was calibrated to measure 61 bands in the range of 430 to 1000 nm at a spatial resolution of 1 m. Georeferencing the TM images to the ETM+ image collected coincident with AISA provided continuity between the two datasets. TM images were corrected for atmospheric effects using the iteratively re-weighted Multivariate Alternation Detection (IR-MAD) technique (Canty & Nielsen, 2008) with a synthetic Landsat image ($AISA_{30}$) serving as reference data. $AISA_{30}$ was produced by spectral resampling the AISA image using ENVI's built-in filter functions and

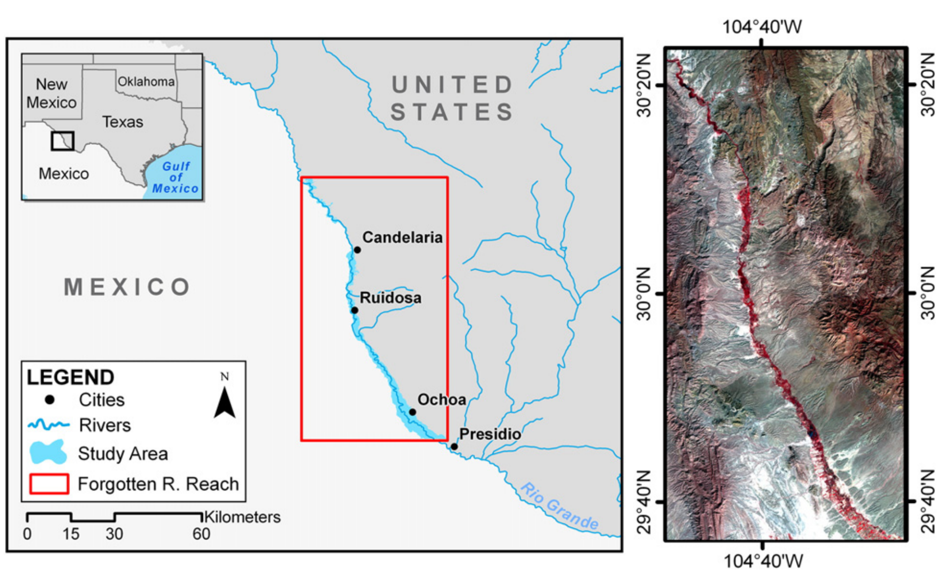

Fig. 1. Location of the study site, the Forgotten River Reach of the Rio Grande. Red false-color composite of cropped Landsat imagery emphasizes the vegetated riparian zone.

spatial resampling the image using an average filter function tool to match the resolution of the Landsat TM images. Spectral subsets (Bands 1–4) of the Landsat TM images were selected to correspond with the spectral range of AISA, as this range has been shown to be effective for saltcedar discrimination (Everitt & DeLoach, 1990). Finally, images were masked to include only the vegetated buffer on either side of the Forgotten River.

3. Methods

The methodology consists of three sequential stages (Fig. 2). In the first stage, the Landsat images are subjected to two soft classification techniques in order to derive sub-pixel fractional cover values for multiple land cover classes. In the second stage, the fractional covers are reclassified into discrete values using the proposed threshold continuum approach. Lastly, landscape metrics are computed to characterize the spatial structure of saltcedar across the landscape. Saltcedar metrics are analyzed across time and also compared to spatial patterns for native woody riparian vegetation to determine if saltcedar landscape structure changes are coupled with corresponding, opposite changes for the native vegetation.

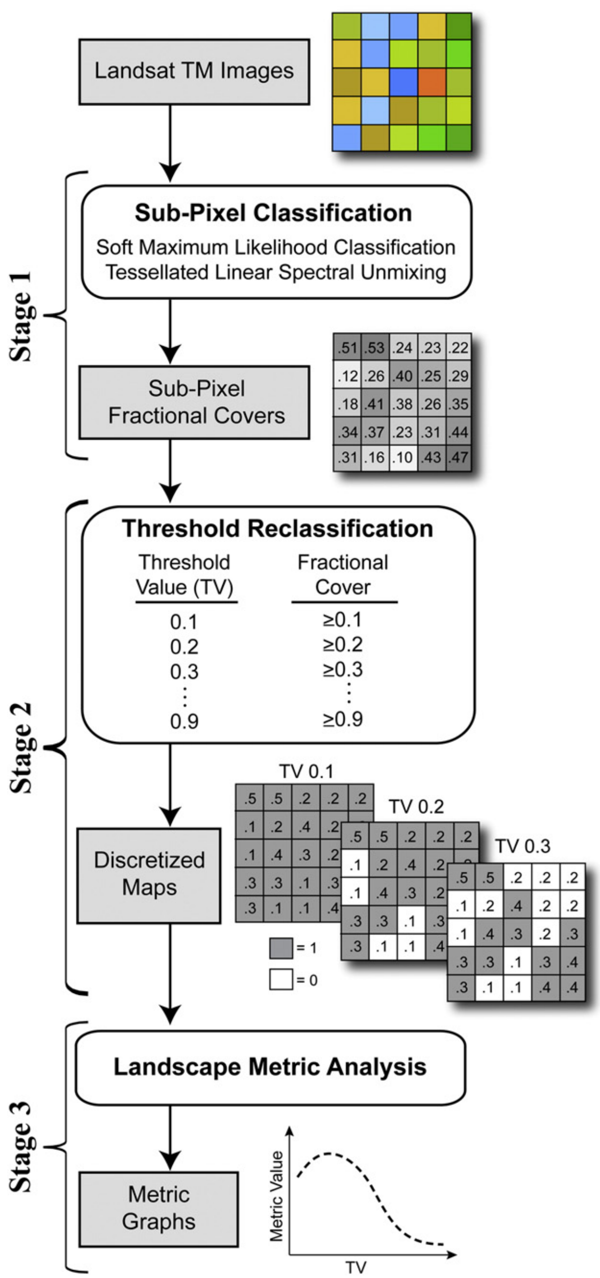

Fig. 2. Three stages of the methodology. At each stage, data are processed (white rectangles) and new datasets are generated (gray rectangles), which form the inputs for the next stage. In Stage I, Landsat TM images are classified using two sub-pixel classification techniques to derive fractional covers. In Stage 2, sub-pixel fractional covers are discretized into nine separate maps, one for each threshold value, and pixels recoded 1 for inclusion, or 0 for exclusion in metric analyses. In Stage 3, discretized maps are subjected to landscape metric analysis.

3.1. Sub-pixel classification

Each Landsat TM image is subjected to two sub-pixel classification techniques to derive fractional land cover values: (1) SMLC and (2) TLSU.

3.1.1. Soft maximum likelihood classification (SMLC)

Maximum likelihood classification (MLC) is the most common supervised classification technique for remote sensing data (Richards & Jia, 1999) and has proven to be the most robust method when spectral information is normally distributed (Bischof et al., 1992). The discriminant function calculated for each pixel maximizes the posterior probability that a pixel belongs to a certain land cover class and assigns each pixel to a single class according to the highest probability.

The posterior probabilities from MLC, which have been shown to be related to land cover proportions in a pixel (Foody et al., 1992; Hill et al., 2007) serve as the fractional land covers in SMLC. In this study, three classes are defined: saltcedar, native woody riparian vegetation (native), and other. We are limited in the number of classes based on the availability of four Landsat TM bands that coincide with the spectral range of AISA. The first two classes are defined by the biological focus of the study to discern saltcedar from all other native woody riparian vegetation species. The third class, other, includes very diverse spectral characteristics and is intended to capture all other types of non-woody vegetation as well as all other non-vegetated land covers. Table 1 lists the specific land covers included in each class.

Training samples were selected from GPS polygons of vegetated areas collected during field campaigns in November 2004 and December 2005. Training samples were verified against the AISA image acquired concurrent with the 2005 field campaign and high resolution aerial photography from 1996, 2004, and 2008 (Texas Water Development Board, 2010). Care was taken to ensure that training pixels selected for the 2000 image did not change land cover class from 1996 to 2004, and it was assumed that these pixels retained their same land cover in 2000. A total of 298, 293, and 379 training pixels were selected for the 2000, 2004, and 2008 images, respectively. From the training samples, SMLC calculates the probability (0.0–1.0) that a pixel belongs to each class with the constraint that the three probabilities, which serve as the fractional land cover values, must be non-negative and sum to one. Accuracy is assessed using the sub-pixel confusion–uncertainty matrix (SCM; Silván-Cárdenas & Wang, 2008) which utilizes a finer resolution image for reference data and does not rely on test samples from the original images. Refer to Section 4.1 for explanation of the accuracy assessment and collection of reference data.

3.1.2. Tessellated linear spectral unmixing (TLSU)

TLSU (Silván-Cárdenas & Wang, 2010) is based on Delaunay tessellations where spectral endmembers form the vertices of a simplex (i.e., a triangle in two-dimensional space, tetrahedron in three-dimensional space, etc.). A mixed pixel is plotted in spectral space, and enclosing endmembers are selected based on spectral proximity to the mixed pixel. The pixel is linearly unmixed as a combination of three endmembers, originating from each of the three

Table 1
Land cover types for the three classes.

Class	Land cover types
Saltcedar	Saltcedar (*Tamarix* spp)
Native woody riparian vegetation	Mesquite (*Prosopis glandulosa*)
	Poverty weed (*Iva axillaris* Pursh)
	Willow (*Salix* spp)
	Gray brush
	Marshy weed (*Limnophila* spp)
	Native bushes
Other	Grasses (all types)
	Creosote bush (*Larrea tridentate)*
	Sand
	Desert gravel
	Paved road
	Roof
	Water (shallow and deep water bodies)
	Wetland

classes: saltcedar, native woody riparian vegetation, and other (see Table 1). Spectral signatures for endmembers were collected during the 2004 and 2005 field campaigns. Unmixing results are reported as non-negative fractions and must sum to one for each pixel. Silván-Cárdenas and Wang (2010) found that TLSU outperforms both unconstrained and fully constrained linear spectral unmixing methods, while non-linear approaches show only marginal improvement but with significant computational burden. TLSU calculations were completed in Matlab technical computing environment (The Mathworks, Inc. 2002) and utilize averaged hyperspectral vegetation measurements obtained from AISA using the ground truth GPS points and polygons for vegetated areas collected during the field campaigns that occurred during the late fall–early winter periods of 2004 and 2005. Additional polygons for non-vegetated endmembers were selected directly on-screen from visual image interpretation.

3.2. Threshold continuum reclassification

The SMLC and TLSU fractional values must be modified before implementing landscape metrics since metrics are only directly compatible with hard classifications. Past studies have employed a range approach to harden soft classifications whereby pixels are grouped based on distinct proportional ranges. Pixels satisfying the criteria at each range are hardened into separate groups for metric analysis (Rashed, 2008; Van de Voorde et al., 2009; Walsh et al., 2008). This approach separates pixels using upper and lower limits and does not consider values above or below the range extent. Reclassifying the data in this manner promotes sporadic, isolated pixels and patches (groups of connected, similar pixels) and can create a 'donut hole' effect (Fig. 3a), which can lead to inaccurate and unreliable metric calculations.

The threshold continuum approach is tested here as an alternative to the range approach and incorporates the continuous spectrum of fractional covers into landscape metric calculations. The threshold approach treats the landscape as a gradually changing gradient and eliminates problems associated with the range approach by aggregating all pixels with values greater than the threshold value and reassigning pixel values through binary reclassification (Fig. 3b). All pixels exceeding a cutoff value are reclassified as 1 and included in the metric calculation. All pixels below the cutoff value are assigned a value of 0 and excluded from metric calculations. This binary reclassification is repeated at each threshold increment. In this way, the landscape is characterized according to a continuum of established minimum proportions of saltcedar that can be related to the degree of invasion.

The main advantage to the threshold approach is that metrics can be compared across the continuum of threshold values to determine how landscape structure is changing as the proportion of saltcedar increases. Additionally, data loss that typically results from discretizing soft classifications is minimized by the ability to set infinitely small threshold increments. Key thresholds can also be identified where spatial patterns show the greatest response to changes in saltcedar proportion. The threshold continuum approach for calculating landscape metrics on sub-pixel data and analyzing those results in terms of vegetation cover changes represents a methodological contribution of this study.

Each of the SMLC and TLSU results was reclassified into nine discrete maps of saltcedar presence–absence using the threshold continuum approach. The nine maps were derived by partitioning the sub-pixel data at nine threshold values set in 0.1 increments from 0.0 to 1.0. All pixels with saltcedar proportions greater than or equal to the threshold break were assigned a value of 1 and all other pixels were assigned 0. For example, when the 0.3 threshold is applied, all

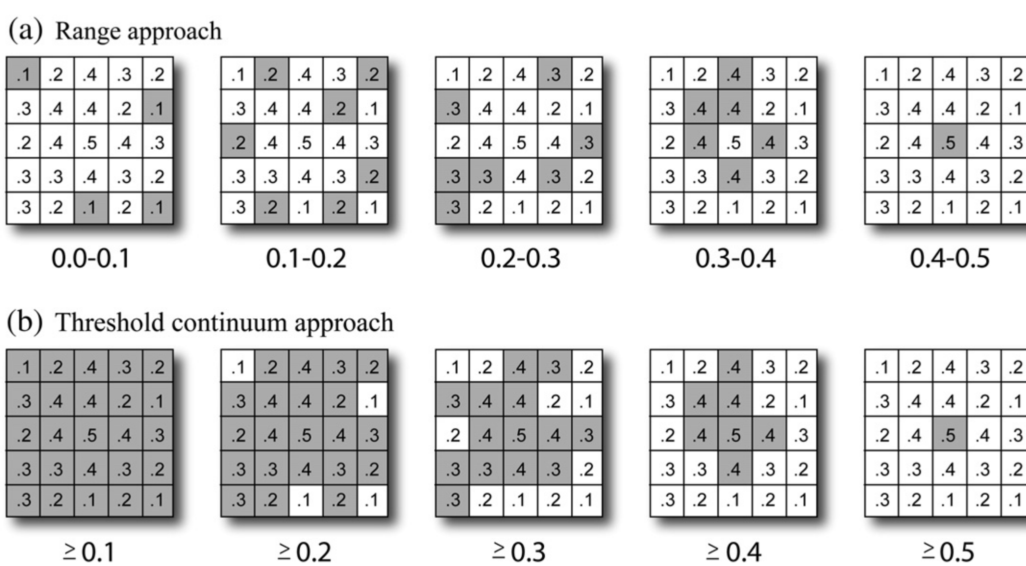

Fig. 3. Examples of discretized maps using (a) the range approach and (b) the threshold continuum approach. Gray pixels satisfy the respective range or threshold criteria, are assigned a value of 1 and are included in metric analyses. White pixels do not satisfy the criteria, are assigned a value of 0 and omitted from metric analyses. The range approach can generate sporadic, isolated pixels (0.0–0.1 and 0.1–0.2), and can produce a 'donut hole' effect (0.3–0.4). The threshold approach generates a more contiguous landscape at each fractional cover value.

pixels with fractional cover of 0.3 and greater are coded 1 (refer to Fig. 2, Stage 2). Pixels with proportions below 0.3 are coded 0 and omitted from metric analyses. In order to eliminate the 0.0 threshold case where every pixel is included and metrics are calculated for one, single, homogeneous patch occupying the entire study area, 0.1 was chosen as the starting threshold.

3.3. Landscape metric analysis

Landscape metrics were calculated using FRAGSTATS 3.3 (McGarigal et al., 2002). FRAGSTATS is a spatial pattern analysis software program that can compute a host of landscape metrics; however, many of these measures are redundant (Tang et al., 2005). The number of patches (NP), patch size coefficient of variation (PSCOV), patch cohesion index (Cohesion), and normalized landscape shape index (nLSI) were chosen to characterize fragmentation, connectedness, and shape complexity. These metrics were selected because they provide insight into the changing spatial patterns of saltcedar with reduced redundancy. A total of 216 metric values were calculated (2 classifications 3 years 9 thresholds 4 metrics = 216 values).

NP (Forman & Godron, 1986; McGarigal & Marks, 1995) is a count of the number of patches at each fractional cover threshold and provides information on fragmentation. Patches are defined here as a contiguous group of pixels based on the eight-neighbor rule. Large NP indicates a fragmented landscape.

$$NP = n_i \tag{1}$$

where

$n =$ the number of patches of class *i*.

PSCOV (McGarigal & Marks, 1995) is a measure of the distribution of area among patches. Large PSCOV indicates less uniformity in size among the patches and therefore usually signifies greater fragmentation. Coefficient values are percentages that are greater than or equal to zero with no upper limit.

$$PSCOV = \frac{PASD}{MNPA}(100) \tag{2}$$

where

$PASD =$ Patch Area Standard Deviation

$$PASD = \sqrt{\frac{\sum_{j=1}^{n}\left[x_{ij} - \left(\frac{\sum_{j=1}^{n} x_{ij}}{n_i}\right)\right]^2}{n_i}} \tag{3}$$

$MNPA =$ Mean Patch Area

$$MNPA = \frac{\sum_{j=1}^{n} x_{ij}}{n_i} \tag{4}$$

and

$n_i =$ the number of patches of class *i*
$x_{ij} =$ area of patch *j* of class *i*.

Cohesion (Schumaker, 1996) measures the physical connectedness of patches at each fractional cover threshold and is computed from patch area and perimeter. It is generally accepted that patches will gradually merge as the proportion of patch cells in the landscape increases, eventually forming one, large, highly-connected patch. Cohesion increases with increasing patch cells until an asymptote is reached near the critical proportion. Above this value, the cohesion index is no longer sensitive to patch configuration (Gustafson, 1998).

$$COHESION = \left[1 - \frac{\sum_{j=1}^{n} p_{ij}}{\sum_{j=1}^{n} p_{ij}\sqrt{a_{ij}}}\right]\left[1 - \frac{1}{\sqrt{A}}\right]^{-1}(100) \tag{5}$$

$p_{ij} =$ the perimeter of patch *i* of class *j* (in terms of the number of cell surfaces)
$a_{ij} =$ the area of patch *i* of class *j* (in terms of the number of cells)
$A =$ the total number of cells in the landscape
$n =$ the number of patches of class *i*.

Cohesion values are unitless and range from 0 to 100. As values approach zero, the patches become increasingly fragmented and less connected. Higher cohesion values indicate a more connected landscape (illustrated in Fig. 4a), however cohesion will equal zero when the landscape consists of a single patch.

The metric nLSI (Patton, 1975; McGarigal & Marks, 1995) measures the aggregation of a particular land cover by quantifying the amount of edge surface relative to the amount that would be present for a landscape with equal size but having a simple geometric shape and no internal edge (McGarigal & Marks, 1995).

$$nLSI = \frac{e_i - \min e_i}{\max e_i - \min e_i} \tag{6}$$

where

$e_i =$ total length of perimeter in terms of the number of cell surfaces
$\min e_i =$ minimum possible total length of perimeter of class *i* in terms of the number of cell surfaces
$\max e_i =$ maximum possible total length of edge perimeter of class *i* in terms of the number of cell surfaces.

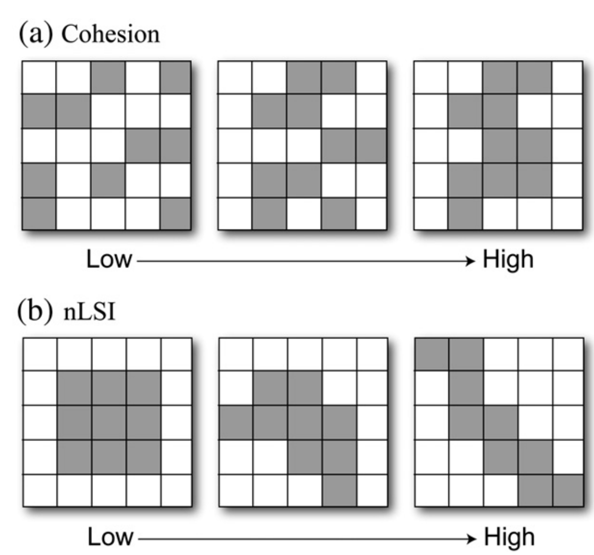

Fig. 4. Conceptual illustration of increasing degrees of (a) cohesion and (b) normalized landscape shape index (nLSI). As cohesion increases, gray pixels become more connected. As nLSI increases, patch shapes become more complex and less compact.

nLSI ranges from 0 to 1 and attains its minimum value, zero, when the patch is completely regular (i.e., a circle or a square). It increases as the patch becomes more complex (Fuller, 2001; O'Neill et al., 1999) with long, thin shapes, being the most complex and having the highest nLSI values (Raines, 2002) (illustrated in Fig. 4b).

Metric results are analyzed across classifications, threshold values, and time in order to interpret the changing spatial patterns of saltcedar in the study area. The three-stage methodology applied to saltcedar is also applied to native woody riparian vegetation in order to compare the two and determine whether native vegetation and saltcedar landscape structure changes in the study area are interrelated. Comparison of the spatial and temporal patterns of saltcedar to those of native vegetation can reveal correlated changes and may provide insight into the process of invasion.

4. Results and discussion

4.1. Sub-pixel unmixing results

Classification results for SMLC and TLSU are shown in Fig. 5. SMLC results display distinct very high (dark red hues) and very low (dark green hues) sub-pixel saltcedar proportions with few pixels classified in intermediate ranges. TLSU results yield considerably more variation in sub-pixel proportions across the landscape, and the three images display a wider range of intermediate red and green tones. Based on field observation, saltcedar is intermixed with native vegetation and occurs in varying proportions as the TLSU results suggest, not solely in dense monocultures as the SMLC results suggest.

Accuracy was assessed using the composite operator proposed by Pontius and Cheuk (2006) and evaluated using SCM (see Silván-Cárdenas & Wang, 2008). Due to the difficulty of collecting ground truth fractional coverage data in the field, SCM relies on reference fractions developed from a finer resolution image, in this case the AISA image. AISA was classified through MLC using training samples from the vegetated GPS polygons collected during the 2004 and 2005 field campaigns. A total of 610, 613, and 610 training pixels were chosen for saltcedar, native woody riparian vegetation, and other, respectively. The large number of training pixels is needed given the 61 spectral bands of AISA. The classification was spatially resampled to 30 m to match the resolution of the TLSU and SMLC classifications, and precise land cover fractions were assigned to each pixel during the resampling process to serve as reference data. A total of 1600 reference pixels were selected and measured against corresponding pixels from the three images. No high resolution satellite imagery is available over the study area for 2000 and 2008, therefore those classifications were assessed using the AISA image. However, the areas selected for the accuracy assessment did not change substantially over the eight-year period, and the accuracy assessment is not expected to be highly impacted by the different image acquisition dates.

Overall, TLSU results were more accurate than SMLC results, with fuzzy kappa coefficients, which are a generalization of the fuzzy classification of the kappa coefficient used for hard classifications (see Silván-Cárdenas & Wang, 2008), of 0.92, 0.94 and 0.92 for the 2000, 2004 and 2008 TLSU classifications, versus 0.83, 0.90 and 0.93 for the same respective SMLC classifications. Based on visual comparison of the classified images combined with field observation and the accuracy assessment, it can be concluded that TLSU is more accurately predicting the spatial extent and sub-pixel proportions of saltcedar in the study area compared to SMLC.

4.2. Discretization

The threshold continuum approach is introduced in this study as an alternative to the range approach for discretizing sub-pixel classifications for metric analyses. A comparison of the range and threshold approaches (Fig. 6) shows major differences in both the number of pixels included at each threshold value and the distribution of pixels across the ranges/threshold values. For the range approach (Fig. 6a), the number of pixels in each of the nine ranges is nearly uniform for both SMLC and TLSU. When pixels are reclassified using the threshold approach (Fig. 6b), all pixels above the threshold value are cumulated. Therefore, a larger number of pixels (and a larger portion of the study area) are analyzed at each threshold value compared to the range method. There is also a continuous, gradual decline in the number of pixels as threshold increases, creating a progressively changing landscape in terms of the number of pixels assessed at each threshold. While the proposed threshold approach improves the method for discretizing sub-pixel data for analysis of invasive species spatial patterns by including a more comprehensive range of fractional covers, it still constitutes a hardening of soft data.

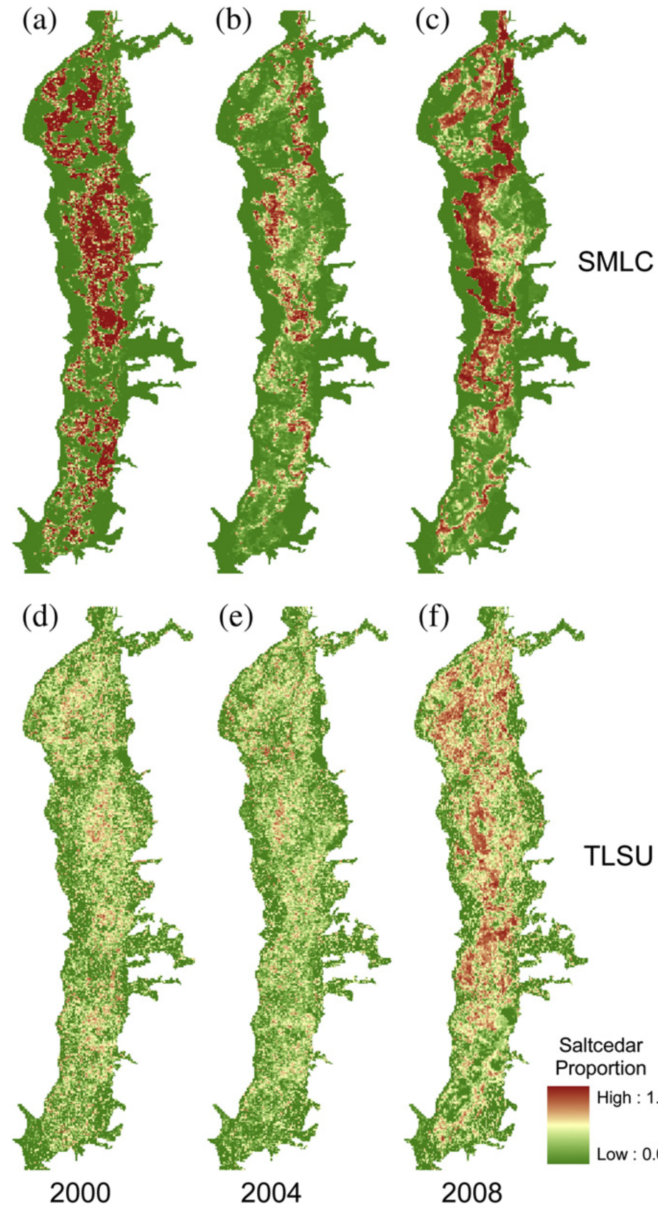

Fig. 5. Saltcedar classification results for (a–c) soft maximum likelihood classification (SMLC) and (d–f) tessellated linear spectral unmixing (TLSU) for a portion of the study area. Dark red pixel indicate high proportions of saltcedar and dark green pixels indicate low proportions.

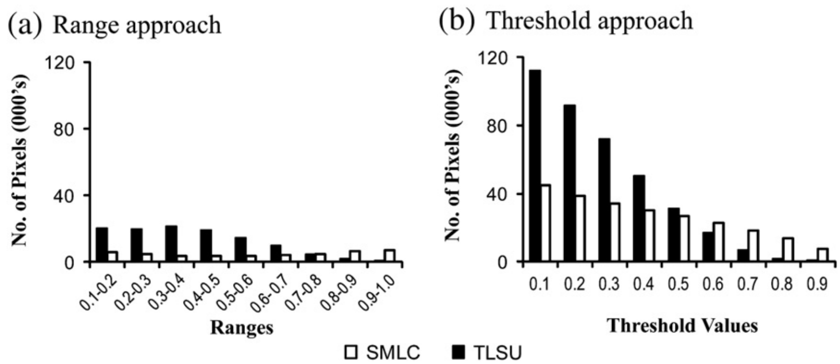

Fig. 6. Comparison of the number of pixels included at each discretization step using (a) the range approach versus and (b) the threshold approach. The range approach produces a nearly uniform distribution of pixels for both the soft maximum likelihood classification (SMLC) and tessellated liner spectral unmixing (TLSU). For the threshold approach, each threshold includes all pixels greater than or equal to the value. Therefore, the number of pixels continuously decreases as threshold increases, and the overall number of pixels is greater since pixels are cumulated at each threshold value. 2008 classifications were used in this comparison, but 2000 and 2004 classifications exhibit similar trends.

Therefore, some inherent sub-pixel detail will ultimately be lost, especially when coarse threshold increments are applied.

Compared to the range approach, the threshold method is more suitable for characterizing the landscape along a continuum of established minimum land cover proportions that can then be related to the degree of invasion or spread of vegetation. However, the range approach does offer benefits for certain types of analyses that are not attainable with the threshold approach. Specifically, in situations where only low or very specific ranges of land cover proportions are desired, the range approach should be utilized. Additionally, when characterizing spatial patterns using the threshold approach, researchers should be aware that for low thresholds, the metrics include a wide variation of land covers and therefore characterize a heterogeneous landscape. For studies seeking to analyze only uniform pixels, the range approach is better suited.

4.3. Spatial pattern analysis

The landscape metric results for the SMLC and TLSU techniques exhibit very different patterns (Fig. 7). In all four metrics tested, SMLC values remain nearly constant across the fractional cover ranges. In contrast, TLSU curves change significantly across thresholds. This indicates that landscape structure varies as sub-pixel proportions are increased. In terms of NP, the TLSU curve (Fig. 7a) peaks at the 0.3 threshold with 5640 patches. The most patches of saltcedar occur at this proportion, and therefore this is the proportion where the landscape is most fragmented. After the peak, the TLSU curve decreases steadily across the remaining thresholds. The corresponding SMLC curve does not show any fluctuations in NP and provides little additional information regarding the state of fragmentation of the landscape at different saltcedar fractional covers. PSCOV also

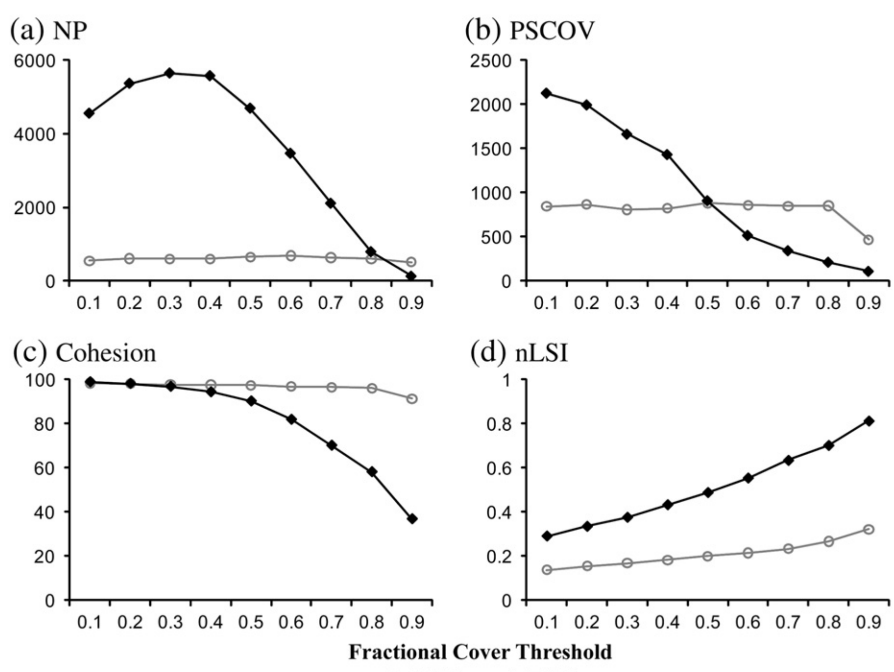

Fig. 7. Metric values for soft maximum likelihood classification (SMLC) and tessellated linear spectral unmixing (TLSU) classification results for saltcedar plotted across the nine fractional cover thresholds for (a) number of patches (NP), (b) patch size coefficient of variation (PSCOV), (c) cohesion, and (d) normalized landscape shape index (nLSI). Metric values are linearly interpolated to produce curves.

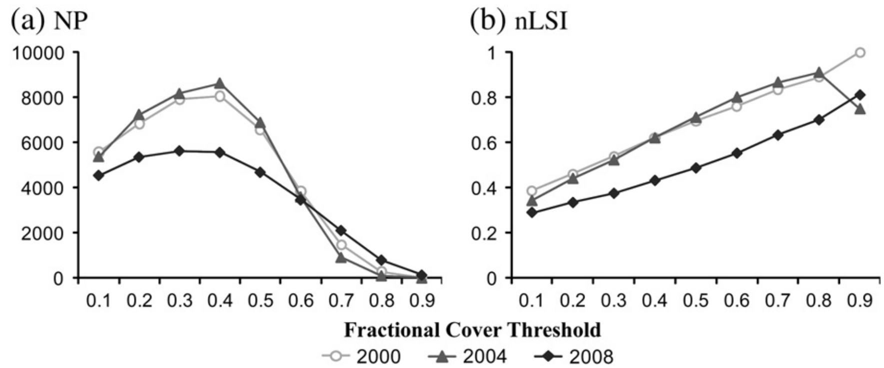

Fig. 8. Comparison of 2000, 2004, and 2008 metric values for saltcedar fractional cover thresholds for (a) number of patches (NP) and (b) normalized landscape shape index (nLSI). Values are calculated using tessellated linear spectral unmixing (TLSU) results and are linearly interpolated to produce curves.

provides insight on fragmentation, and TLSU curves are again more variable than SMLC curves (Fig. 7b). TLSU values decline across the thresholds and range from a maximum of 2125 to a minimum of 107. High PSCOV values for TLSU at low thresholds gives further evidence that the landscape is most fragmented at low saltcedar proportions. Values for SMLC range from 865 to 465 with minimal fluctuations aside from a slight drop at the 0.9 threshold.

Cohesion results (Fig. 7c) follow the same trends seen thus far: TLSU curves vary across the thresholds while SMLC curves remain stable. The TLSU curve reaches a plateau at approximately the 0.3 threshold. This point where the asymptote is reached is referred to as the critical threshold and signifies the cohesion index is no longer sensitive to patch configuration (see Section 3.3). At thresholds below 0.3, the TLSU results are not sensitive to landscape cohesion. However, TLSU is sensitive to changes across most of the threshold increments and provides information on the varying degree of landscape connectedness as sub-pixel proportion increases. The SMLC asymptote is reached at 0.8, which implies that SMLC results are only sensitive to patch connectedness at the highest proportion of saltcedar.

The nLSI curves for TLSU and SMLC are similar in shape (Fig. 7d), but TLSU values span a larger range (0.29–0.81 versus 0.14–0.32 for SMLC) signifying that patch shape complexity for TLSU changes more extensively as threshold increases.

Metric results presented in Fig. 7 are for the 2008 dataset, however similar patterns were observed for the 2000 and 2004 datasets. In general, metrics for SMLC results are less responsive to changes in fractional cover than TLSU and demonstrate only minor variations across the threshold continuum. The greater variation in metrics derived from TLSU is likely because TLSU is formulated to consider intra-class spectral endmembers when unmixing each pixel and is not limited to the three general classes. TLSU has showed superior performance to other linear mixture methods in deconstructing each pixel into its precise combination of land covers, a result that is attributed to the intra-class variability of spectral signatures (Silván-Cárdenas & Wang, 2010). This improved accuracy is propagated into the spatial pattern results, and the metrics based on TLSU classifications consequentially capture more variation in the landscape structure.

Critical thresholds, or points where the shape and slope of the curves change, also provide insight regarding indicative proportions at which significant landscape changes occur. From the results presented in Fig. 7, these critical thresholds occur consistently between 0.3 and 0.7 for each metric. This pattern in the location of critical thresholds is an interesting finding of this research and may prove useful in isolating the land cover proportions that affect the greatest changes in landscape structure. Further investigation is needed to determine the specific optimal fractional cover thresholds or threshold ranges for each metric, but this is a promising area for future research.

Based on the interpretation of the SMLC and TLSU results, unmixing methods can have varying effects on associated metrics. For SMLC, we observed very little change across fractional cover thresholds, while for TLSU we uncovered considerable fluctuations in metric results. Since results show that the unmixing method can affect metric calculations differently, it is necessary to perform unmixing prior to metric calculations as the value of the metric can change drastically based on mixture method and sub-pixel fractional values.

This study is the first instance of landscape metrics being calculated across a continuum of fractional cover thresholds, and the two classifications tested, SMLC and TLSU, responded very differently to metric calculations. Therefore, it is unknown how other types of mixture methods will respond to threshold-based metrics. Additionally, curves are interpreted based on extant studies subjecting remote sensing classifications to landscape metrics. However, since fine threshold increments may produce fine variations in metric values, these curves may warrant more specific interpretation criteria in the future.

4.4. Temporal change

TLSU results were examined in depth to characterize saltcedar distribution changes over time (Fig. 8). NP results for 2000 and 2004 (Fig. 8a) show only slight differences in metric values. However, for the 2008 curves, there are substantial decreases in NP at low thresholds and slight increases in NP at high thresholds when compared to 2004 values. Since the total area of saltcedar increased from 3273 ha in 2004 to 4032 ha in 2008 (Table 2), it can be inferred that over time saltcedar has amalgamated many smaller patches into fewer, larger patches, thus decreasing overall saltcedar densities. Above the 0.6 threshold, NP values increase between 2004 and 2008 indicating saltcedar has propagated high density patches over time. Given the ability of saltcedar to outcompete native vegetation, along with its areal spread over time, it is reasonable to assume the increase in the number of patches at high thresholds is due to the formation of high-density stands and does not result from the fragmentation of a few large patches into many, smaller patches.

Table 2
Change in area (ha) over time for the three classes.

Class	2000	2004	2008	Overall change
Saltcedar	3094	3273	4032	+938
Native woody riparian vegetation	3667	3303	3566	−102
Other	13,831	14,016	12,994	−837

Normalized LSI, which provides information on the complexity of patch shape, increases across thresholds for all years (Fig. 8b), but 2008 values are slightly lower than 2000 and 2004 values. High nLSI values correspond to increasingly complex landscape shapes (e.g., longer, thinner riparian zones adjacent to the river). Therefore the rise in complexity as threshold increases implies that the densest saltcedar stands are likely located along river banks. This outcome is supported by prior findings that saltcedar exploits bare, moist, exposed sites with high water availability, such as river banks (Di Tomaso, 1998; Everitt, 1980; Shafroth et al., 2005), and the resilience and rooting abilities of saltcedar allow it to form monotypic stands in those riparian zones (Hart et al., 2005). Lower nLSI values in 2008 can be interpreted as the result of dense cover stands expanding beyond the immediate riparian zone and forming more compact shaped patches as they extend away from the river edge.

Fig. 9 provides examples of the changing saltcedar spatial configurations over time at various small plots across the study area. From 2000 to 2004, the number of pixels with high saltcedar proportions increases slightly in each of the plots, and compact groupings are starting to form. In 2008, there are prominent formations of high density saltcedar patches, and large, compact groupings of pixels with high saltcedar proportions are easily observed. These examples verify metric results (see Fig. 8) which showed small changes between 2000 and 2004 and more substantial differences in 2008. The examples in Fig. 9 also support the inferences drawn from the metric results that saltcedar is forming high density, compact patches over time.

4.5. Correlated class structure patterns

Prior research suggests that the changing spatial extent of saltcedar is coupled with the displacement of native vegetation. Comparison of native and saltcedar class metrics can aid in supporting this theory and may reveal where such transitions are occurring. Based on the TLSU classification results, from 2000 to 2008 native woody riparian vegetation saw a net loss of 102 ha while saltcedar gained 938 ha (Table 2). These results are consistent with field knowledge that saltcedar is outcompeting and displacing native vegetation in the study area. The third class, other, accounts for disagreement in area change between saltcedar and native vegetation.

Metric results for the two classes (Fig. 10) also corroborate prior field knowledge that saltcedar is displacing native vegetation. Although NP values (Fig. 10a) for native are higher than those for saltcedar at high thresholds (0.7 and above), there is less total area overall for native (3566 ha of native versus 4032 ha of saltcedar). Therefore, the larger number of native patches at high thresholds indicates greater fragmentation, and the increase in patches is not due to a greater amount of native woody riparian vegetation.

According to nLSI values, saltcedar patches are more complex than native patches at mid and high thresholds (above 0.3). Previous findings from this research established that the highest density patches of saltcedar are likely located along the river and that saltcedar is expanding away from the river and forming a greater number of contiguous, high-density patches. Comparison of native and saltcedar nLSI values supports these findings as the highest density saltcedar patches are more likely to occupy areas along the river than native patches of comparable density because saltcedar patches have higher nLSI values. Contrasting the expansion and occupation along the river of saltcedar to the fragmentation and decline in area of native vegetation, it can be inferred that saltcedar is outcompeting native vegetation along the riparian zone.

It should be noted that while spatial patterns can be inferred from landscape metrics, the metrics themselves do not provide spatially

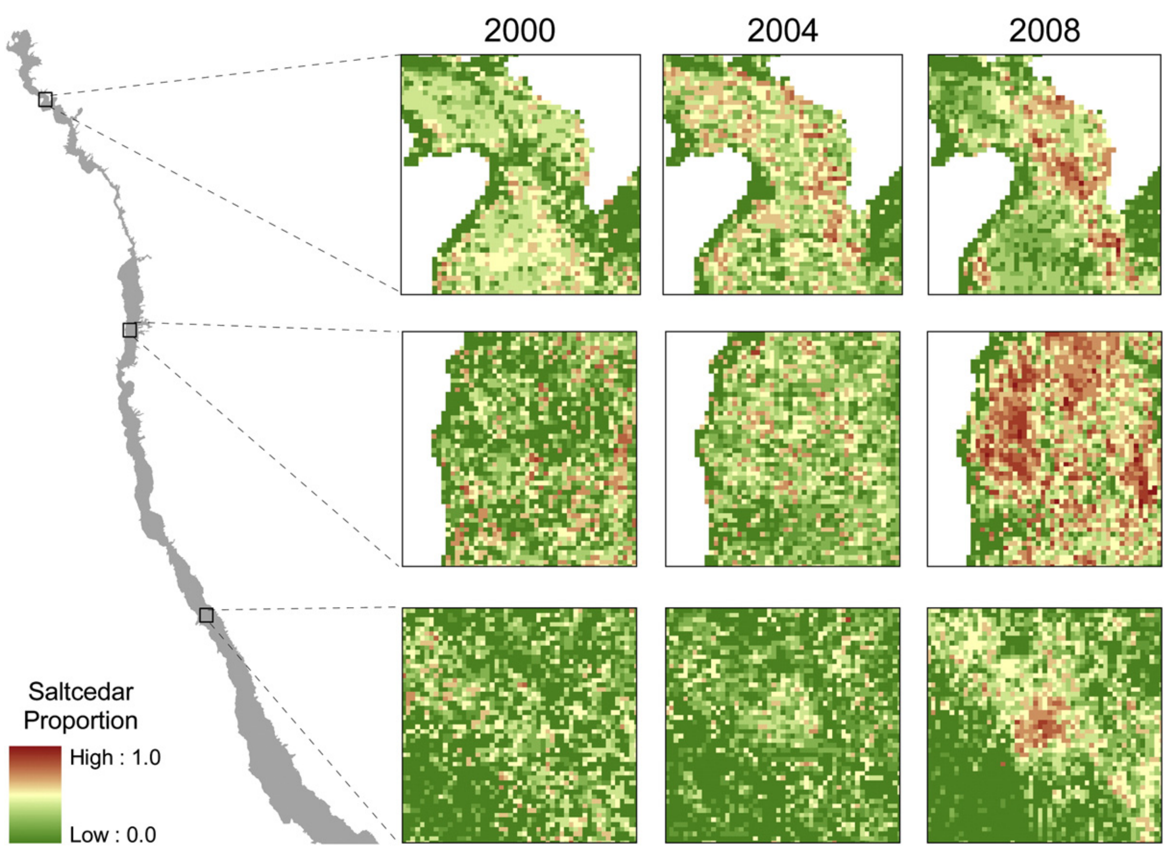

Fig. 9. Examples showing the information of high fractional cover saltcedar patches over time for three different parts of the study area. Red pixels indicate high saltcedar proportions and green pixels indicate low proportions. Subtle changes are apparent between 2000 and 2004 as red pixels begin to cluster. In the 2008 images, dense areas of high proportion pixels are evident.

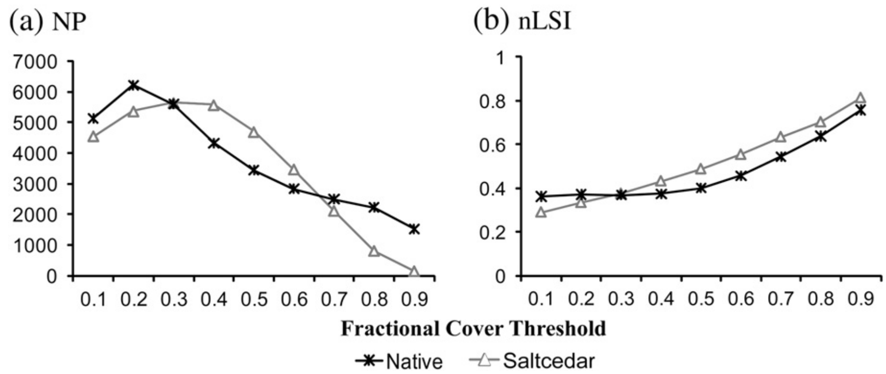

Fig. 10. Comparison of metric values for (a) number of patches (NP) and (b) normalized landscape shape index (nLSI) for native woody riparian vegetation (native) and saltcedar. Values are derived from the 2008 tessellated linear spectral unmixing (TLSU) classification results and are linearly interpolated to produce curves.

referenced results. Therefore, spatial interpretation of landscape metrics depends on inferences of each measure in the context of regional knowledge and an understanding that values may differ in structurally different landscapes (Hargis et al., 1998).

Saltcedar is one of the most threatening invasive species in the southwestern U.S. (Hamada et al., 2007; Wang & Silván-Cárdenas, under revision) and is a high priority species for control efforts (Morisette et al., 2006). Quantifying the spatial and temporal distribution patterns through landscape metrics can shed light on the process of invasion and help inform ecosystem management decisions. Through testing and applying the threshold continuum approach, we found that metric results can vary significantly across the landscape depending on sub-pixel fractional cover values. Spatial interpretation of metric results indicate that saltcedar is expanding away from the immediate river zone and is forming a greater number of high-density patches and outcompeting native vegetation, especially along the river. These findings would not have been possible using traditional approaches for implementing landscape metrics for remote sensing classifications.

5. Conclusions

Landscape metrics are an attractive tool for quantifying spatial patterns from remote sensing classifications, but they have not been properly exploited to characterize saltcedar invasion. This is likely because metrics cannot be computed directly for fractional cover maps, which are the most viable option to obtain detailed saltcedar infestation information using remotely sensed images. This research tests a new technique for discretizing sub-pixel classifications for metric analysis using a threshold continuum approach that converts continuous fractional cover to discrete classes at gradually increasing thresholds based on cumulated sub-pixel fractional cover. The study tests the threshold approach for several soft classifications of saltcedar along the Forgotten River Reach of the Rio Grande. The proposed threshold method is more suitable for invasive species studies than conventional approaches for discretization since landscape information can be characterized according to the magnitude of invasion. After examining the fractional cover classes using landscape metrics (i.e., NP, PSCOV, Cohesion and nLSI), we interpreted the spatial pattern results in the context of the study area.

The findings of this research include:

(1) Spectral unmixing methods are appropriate for discerning saltcedar in the study area, but results are variable depending on the classification scheme utilized. TLSU outperformed SMLC in terms of more accurately classifying a continuous distribution of saltcedar across the landscape, a characteristic of the study area that has been confirmed by field observation.
(2) Spectral unmixing should be performed prior to metric analysis as metric results can be sensitive to changes in fractional cover.
(3) Over time, saltcedar stands are becoming less fragmented and more compact in shape at higher sub-pixel proportions indicating expansion of saltcedar invasion from the riparian zone.
(4) Saltcedar is displacing native woody riparian vegetation over time and space.

The results from this study can be used to inform ecosystem management decisions regarding saltcedar eradication. Dense saltcedar patches are expanding away from the river, and targeting only the immediate riparian zone through eradication strategies is not effective for saltcedar remediation. Additionally, low threshold patches of saltcedar have become more spatially cohesive over time suggesting a wider overall areal extent of saltcedar distribution. However, these low threshold patches of saltcedar also include a mix of native vegetation and other land covers and therefore must be treated with caution. For instance, aerially spraying herbicides to these areas will blanket the region and not only exterminate saltcedar bushes but also may negatively affect native vegetation.

There are several areas for future work arising from this study. Further testing of a variety of unmixing techniques should be completed to determine whether additional methods exhibit variable curves, such as was seen with the TLSU results, or whether they produce only minor fluctuations across thresholds, as with the SMLC results. Additionally, since metrics are sensitive to sub-pixel fractional cover and do not change linearly over time, future work should include analysis of the rates of change at various thresholds to determine if there are significant factors operating on the landscape at specific land cover proportions and whether optimal thresholds for landscape characterization can be identified.

Acknowledgments

This study was partially supported by grants to Le Wang from the National Science Foundation (DEB-0810933 and BCS-0822489) and from the US Department of Agriculture CSREES Award 2004-38899-02181.

References

Affre, L., Suehs, C., Charpentier, S., Vilà, M., Brundu, G., Lambdon, P., et al. (2010). Consistency in the habitat degree of invasion for three invasive plant species across Mediterranean islands. *Biological Invasions*, *12*(8), 2537–2548.
Bekker, M., Clark, J., & Jackson, M. (2009). Landscape metrics indicate differences in patterns and dominant controls of ribbon forests in the Rocky Mountains, USA. *Applied Vegetation Science*, *12*(2), 237–249.
Bischof, H., Schneider, W., & Pinz, A. (1992). Multispectral classification of Landsat-images using neural networks. *IEEE Transactions on Geoscience and Remote Sensing*, *30*(3), 482–490.

Brown, D., Duh, J., & Drzyzga, S. (2000). Estimating error in an analysis of forest fragmentation change using North American Landscape Characterization (NALC) data. *Remote Sensing of Environment*, *71*(1), 106–117.

Canty, M., & Nielsen, A. (2008). Automatic radiometric normalization of multitemporal satellite imagery with the iteratively re-weighted MAD transformation. *Remote Sensing of Environment*, *112*(3), 1025–1036.

deWinton, M., & Clayton, J. (1996). The impact of invasive submerged weed species on seed banks in lake sediments. *Aquatic Botany*, *53*(1–2), 31–45.

Di Tomaso, J. (1998). Impact, biology, and ecology of saltcedar (*Tamarix* spp.) in the southwestern United States. *Weed Technology*, *12*(2), 326–336.

Dukes, J., & Mooney, H. (2004). Disruption of ecosystem processes in western North America by invasive species. *Revista Chilena De Historia Natural*, *77*(3), 411–437.

Everitt, B. (1980). Ecology of Saltcedar — Plea for research. *Environmental Geology*, *3*(2), 77–84.

Everitt, J., & Deloach, C. (1990). Remote-sensing of Chinese tamarisk (*Tamarix chinensis*) and associated vegetation. *Weed Science*, *38*(3), 273–278.

Everitt, J., Escobar, D., Alaniz, M., Davis, M., & Richerson, J. (1996). Using spatial information technologies to map Chinese tamarisk (*Tamarix chinensis*) infestations. *Weed Science*, *44*(1), 194–201.

Foody, G., Campbell, N., Trodd, N., & Wood, T. (1992). Derivation and applications of probabilistic measures of class membership from the maximum-likelihood classification. *Photogrammetric Engineering and Remote Sensing*, *58*(9), 1335–1341.

Forman, R., & Godron, M. (1986). *Landscape ecology.* USA: John Wiley and Sons, Inc.

Fuller, D. (2001). Forest fragmentation in Loudoun County, Virginia, USA evaluated with multitemporal Landsat imagery. *Landscape Ecology*, *16*(7), 627–642.

Groeneveld, D., & Watson, R. (2008). Near-infrared discrimination of leafless saltcedar in wintertime Landsat TM. *International Journal of Remote Sensing*, *29*(12), 3577–3588.

Gustafson, E. (1998). Quantifying landscape spatial pattern: What is the state of the art? *Ecosystems*, *1*(2), 143–156.

Hamada, Y., Stow, D., Coulter, L., Jafolla, J., & Hendricks, L. (2007). Detecting *Tamarisk* species (*Tamarix* spp.) in riparian habitats of Southern California using high spatial resolution hyperspectral imagery. *Remote Sensing of Environment*, *109*(2), 237–248.

Hargis, C., Bissonette, J., & David, J. (1998). The behavior of landscape metrics commonly used in the study of habitat fragmentation. *Landscape Ecology*, *13*(3), 167–186.

Harold, M., Couclelis, H., & Clarke, K. (2005). The role of spatial metrics in the analysis and modeling of urban land use change. *Computers, Environment and Urban Systems*, *29*, 369–399.

Hart, C., White, L., McDonald, A., & Sheng, Z. (2005). Saltcedar control and water salvage on the Pecos River, Texas, 1999–2003. *Journal of Environmental Management*, *75*(4), 399–409.

Hill, R., Granica, K., Smith, G., & Schardt, M. (2007). Representation of an alpine treeline ecotone in SPOT 5 HRG data. *Remote Sensing of Environment*, *110*, 458–467.

Kamusoko, C., & Aniya, M. (2007). Land use/cover change and landscape fragmentation analysis in the Bindura District, Zimbabwe. *Land Degradation & Development*, *18*(2), 221–233.

Keshava, N., & Mustard, J. (2002). Spectral unmixing. *IEEE Signal Processing Magazine*, *19*(1), 44–57.

Mas, J., Gao, Y., & Pacheco, J. (2010). Sensitivity of landscape pattern metrics to classification approaches. *Forest Ecology and Management*, *259*(7), 1215–1224.

McGarigal, K., Cushman, S., Neel, M., & Ene, E. (2002). FRAGSTATS: Spatial pattern analysis program for categorical maps. Computer software program produced by the authors at the University of Massachusetts, Amherst. Retrieved from. http://www.umass.edu/landeco/research/fragstats/fragstats.html

McGarigal, K., & Marks, B. (1995). FRAGSTATS: Spatial pattern analysis program for quantifying landscape structure. *U S Forest Service General Technical Report PNW*, *0*(351), I–122.

Morisette, J., Jarnevich, C., Ullah, A., Cai, W., Pedelty, J., & Gentle, J. (2006). A tamarisk habitat suitability map for the continental United States. *Frontiers in Ecology and the Environment*, *4*(1), 11–17.

Narumalani, S., Mishra, D., Wilson, R., Reece, P., & Kohler, A. (2009). Detecting and mapping four invasive species along the floodplain of North Platte River, Nebraska. *Weed Technology*, *23*(1), 99–107.

O'Neill, R., Riitters, K., Wickham, J., & Jones, K. (1999). Landscape pattern metrics and regional assessment. *Ecosystem Health*, *5*(4), 225–233.

Patton, D. (1975). A diversity index for quantifying habitat 'edge'. *Wildlife Society Bulletin*, *3*, 171–173.

Pontius, R., & Cheuk, M. (2006). A generalized cross-tabulation matrix to compare soft-classified maps at multiple resolutions. *International Journal of Geographical Information Science*, *20*(1), 1–30.

Pu, R., Gong, P., Tian, Y., Miao, X., Carruthers, R., & Anderson, G. (2008). Using classification and NDVI differencing methods for monitoring sparse vegetation coverage: a case study of saltcedar in Nevada, USA. *International Journal of Remote Sensing*, *29*(14), 3987–4011.

Raines, G. (2002). Description and comparison of geologic maps with FRAGSTATS — A spatial statistics program. *Computers & Geosciences*, *28*(2), 169–177.

Rashed, T. (2008). Remote sensing of within-class change in urban neighborhood structures. *Computers Environment and Urban Systems*, *32*(5), 343–354.

Richards, J., & Jia, X. (1999). *Remote sensing digital image analysis* (3rd Edition). Berlin: Springer-Verlag.

Roberts, D., Gardner, M., Church, R., Ustin, S., Scheer, G., & Green, R. (1998). Mapping chaparral in the Santa Monica Mountains using multiple endmember spectral mixture models. *Remote Sensing of Environment*, *65*(3), 267–279.

Schumaker, N. (1996). Using landscape indices to predict habitat connectivity. *Ecology*, *77*, 1210–1225.

Shafroth, P., Cleverly, J., Dudley, T., Taylor, J., Van Riper, C., & Weeks, E. (2005). Control of *Tamarix* in the Western United States: Implications for water salvage, wildlife use, and riparian restoration. *Environmental Management*, *35*(3), 231–246.

Silván-Cárdenas, J., & Wang, L. (2008). Sub-pixel confusion–uncertainty matrix for assessing soft classifications. *Remote Sensing of Environment*, *112*(3), 1081–1095.

Silván-Cárdenas, J., & Wang, L. (2010). Retrieval of subpixel *Tamarix* canopy cover from Landsat data along the Forgotten River using linear and nonlinear spectral mixture models. *Remote Sensing of Environment*, *114*(8), 1777–1790.

Song, C. (2005). Spectral mixture analysis for subpixel vegetation fractions in the urban environment: How to incorporate endmember variability? *Remote Sensing of Environment*, *95*(2), 248–263.

Soto, I., Andrefouet, S., Hu, C., Muller-Karger, F., Wall, C., & Sheng, J. (2009). Physical connectivity in the Mesoamerican Barrier Reef System inferred from 9 years of ocean color observations. *Coral Reefs*, *28*(2), 415–425.

Southworth, J., Munroe, D., & Nagendra, H. (2004). Land cover change and landscape fragmentation — Comparing the utility of continuous and discrete analyses for a western Honduras region. *Agriculture Ecosystems & Environment*, *101*(2–3), 185–205.

Tang, J., Wang, L., & Zhang, S. (2005). Investigating landscape pattern and its dynamics in Daqing, China. *International Journal of Remote Sensing*, *26*(11), 2259–2280.

Texas Water Development Board (2010). Digital ortho quarter quad imagery. Retrieved from Texas Natural Resources Information System. http://www.tnris.state.tx.us/

Van de Voorde, T., Canters, F., van der Kwast, J., Engelen, G., Binard, M., & Cornet, Y. (2009). Quantifying intra-urban morphology of the Greater Dublin area with spatial metrics derived from medium resolution remote sensing data. *Proceeding of the IEEE 2009 Urban Remote Sensing Joint Event, Shanghai*.

Vitousek, P., Dantonio, C., Loope, L., Rejmanek, M., & Westbrooks, R. (1997). Introduced species: A significant component of human-caused global change. *New Zealand Journal of Ecology*, *21*(1), 1–16.

Walsh, S., McCleary, A., Mena, C., Shao, Y., Tuttle, J., & Gonzalez, A. (2008). QuickBird and Hyperion data analysis of an invasive plant species in the Galapagos Islands of Ecuador: Implications for control and land use management. *Remote Sensing of Environment*, *112*(5), 1927–1941.

Wang, L., & Silván-Cárdenas, J. (under revision). Invasive Saltcedar spread mapping using multi-resolution remote sensing data. *Professional Geographer*.